arXiv:1909.13505

Understanding the Discrepancy between IRX and Balmer Decrement in Tracing Galaxy Dust Attenuation

Jianbo Qin,[1,2] Xian Zhong Zheng,[1] Stijn Wuyts,[3] Zhizheng Pan,[1] and Jian Ren[1,2]

[1]Purple Mountain Observatory, Chinese Academy of Sciences, 10 Yuanhua Road, Nanjing 210033, China
[2]School of Astronomy and Space Sciences, University of Science and Technology of China, Hefei 230026, China
[3]Department of Physics, University of Bath, Claverton Down, Bath, BA2 7AY, UK

ダスト吸収のプローブ
- UV slope (beta) : ageと縮退している。"skin effect"(表面しか見ていないバイアス)の影響を受ける
- Balmer decrement (Ha/Hb)
- IRX (L_UV/L_IR)

とはいえ、Balmer decrementとIRXが一致しないことも多い
- IRXが一定のサンプルを取ると、Balmer decrementは星質量とともに増加する (Koyama +19)
- Balmer decrement一定のサンプルではそんなことは起こらない

データ: 32000銀河(SDSS/GALEX/WISE)

結論: SSFR面密度に依存する。

$$R_{\rm EBV} = 0.79 + 0.15\log({\rm SSFR}/R_{\rm e}^2)$$

$$R_{\rm EBV} \equiv E(B-V)_{\rm IRX}/E(B-V)_{\rm H\alpha/H\beta},$$

- gas metallicityには依存しない
- SSFR面密度が下がるとBalmer decrementから出したダスト吸収量はglobalな星の吸収に比べて相対的に大きくなってしまう
- ダスト吸収を相対的に受けていない中間質量星が増えることに対応しているのだろう
- SSFR面密度がわかれば、balmer decrementから星の吸収の変換をすべきか。

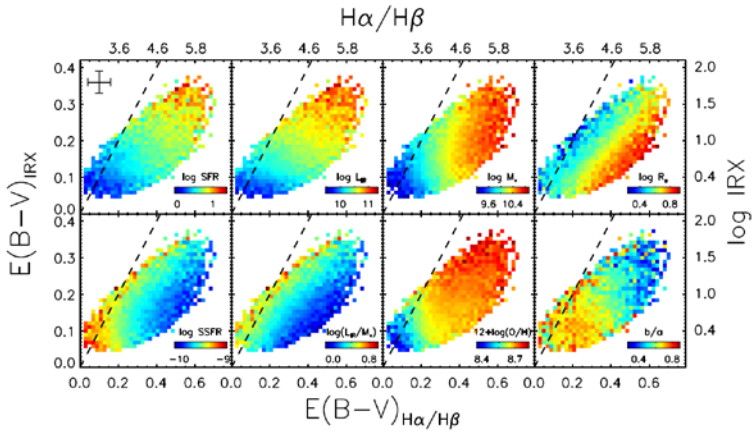

Figure 1. Comparison between $E(B-V)_{\rm H\alpha/H\beta}$ and $E(B-V)_{\rm IRX}$ for our sample of 32354 local SFGs. The top- and right-axis show the equivalent Hα/Hβ and IRX, respectively. We divide each panel into 40×40 sub-grids and color code sub-grids using the median of data points in a given parameter. Here we only count the sub-grids containing >5 SFGs. In these panels from left to right and top to bottom, the parameter used for color coding are SFR, $L_{\rm IR}$, M_*, R_e, SSFR, $L_{\rm IR}/M_*$, 12+log(O/H) and b/a, respectively. The dotted lines mark the relation of $E(B-V)_{\rm IRX} = E(B-V)_{\rm H\alpha/H\beta}$ (i.e., $R_{\rm EBV}=1$). The error bars in the top-left panel show the typical observational uncertainties.

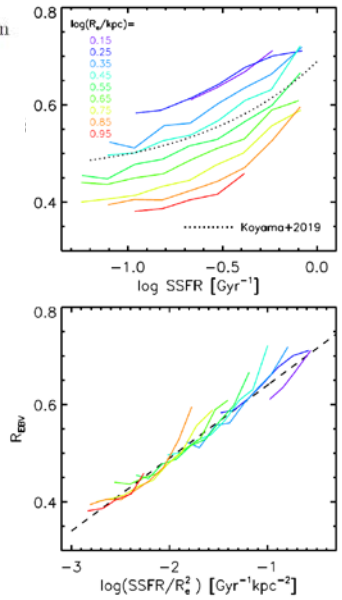

Figure 3. Top panel: the SSFR−$R_{\rm EBV}$ relation as a function of R_e. Solid lines link the median data points of SSFR−$R_{\rm EBV}$ subsamples split by R_e (color-coded). The dotted line is the averaged SSFR−$R_{\rm EBV}$ relation given in Koyama et al. (2019). Bottom panel: the relations between $R_{\rm EBV}$ and SSFR/R_e^2. Color coding is the same as in the top panel. The black dashed line marks the best-fit relation given in Equation 4.

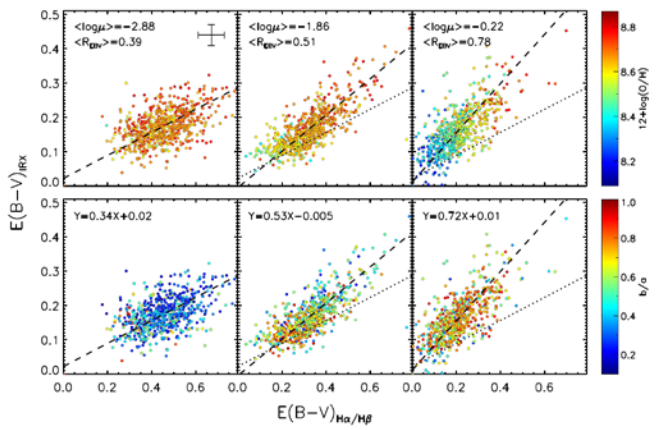

Figure 4. Comparison between $E(B-V)_{\rm H\alpha/H\beta}$ and $E(B-V)_{\rm IRX}$ for three subsamples of local SFGs with different μ (=SSFR/R_e^2). The subsamples are selected from 0%–2% (left), 49%–51% (middle), 98%–100% (right) of the cumulative distribution of μ, respectively. The median μ and $R_{\rm EBV}$ in each bin is labeled. The dashed lines represent the best-fit line $Y = kX + b$ to the data points. The dotted lines in the middle and right panels are the best-fit line in the left panel for comparison. The error bars in the top-left panel show the typical observational uncertainties. Gas-phase metallicity (top panels) and axial ratio (bottom panels) are used to color code data points. At fixed $\log\mu$, the data do not reveal any residual dependence on these parameters.

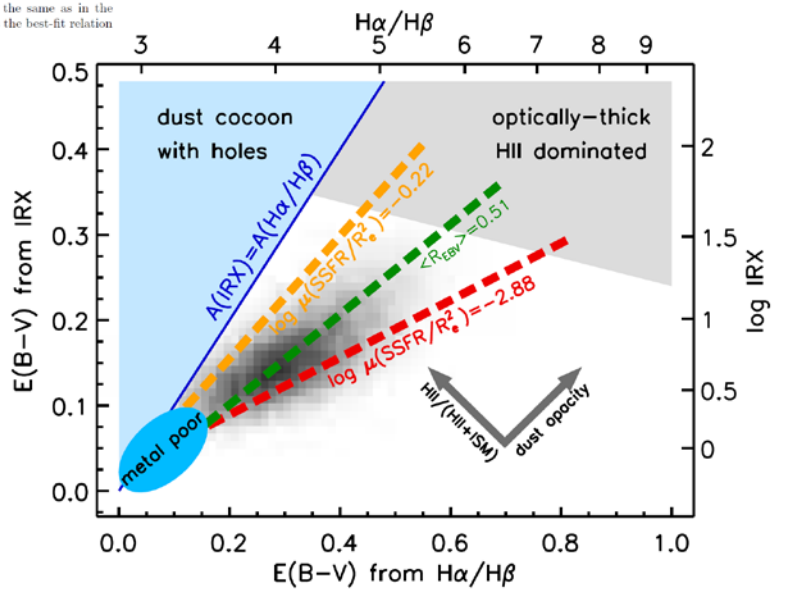

Figure 5. Schematic diagram of dust attenuation of SFGs probed by Hα/Hβ versus by IRX. The background gray scale represents the distribution of our local 32354 SFGs. The yellow, green and red dashed lines represent the best-fit relations to the three subsamples with $\log\mu = -2.88$, -1.86 and -0.22, respectively, presented in Figure 4. SFGs with increasing μ or SSFR/R_e^2 form a steeper Hα/Hβ–IRX relation and yield a higher $R_{\rm EBV}$. The increase of $R_{\rm EBV}$ is likely coupled with the increasing fraction of UV emission from H II regions over the total at higher SSFR, as well as the increasing opacity in the diffuse ISM driven by the decreasing galaxy size. When $R_{\rm EBV}$=1, H II regions dominate the parent galaxies and the global dust attenuation is dominated by that in the H II regions. At a fixed SSFR/R_e^2, the Hα/Hβ–IRX relation is driven by the observed dust attenuation that is regulated by SFR compactness, metallicity and inclination.